Electronic Supplementary Material (ESI) for RSC Advances.


**Electronic Supplementary Information**

# Separation of main and satellite droplets in a deterministic lateral displacement microfluidic device

Naotomo Tottori,[a] Takeshi Hatsuzawa[b] and Takasi Nisisako[b]

[a] *Department of Mechanical Engineering, School of Engineering, Tokyo Institute of Technology, Yokohama, Japan*

[b] *Laboratory for Future Interdisciplinary Research of Science and Technology (FIRST), Institute of Innovative Research, Tokyo Institute of Technology, Yokohama, Japan*

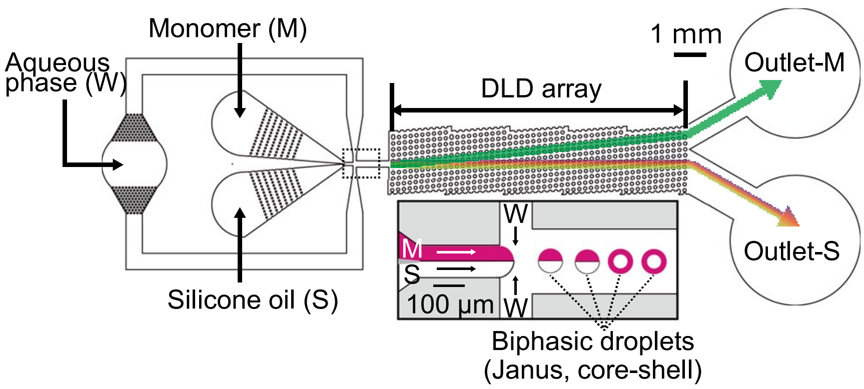


**Fig. S1** Schematic diagram of a hydrophilic single-step DLD array for separation of biphasic main and satellite droplets. The dashed rectangle corresponds to the magnified view of the microfluidic droplet generator (MFDG).

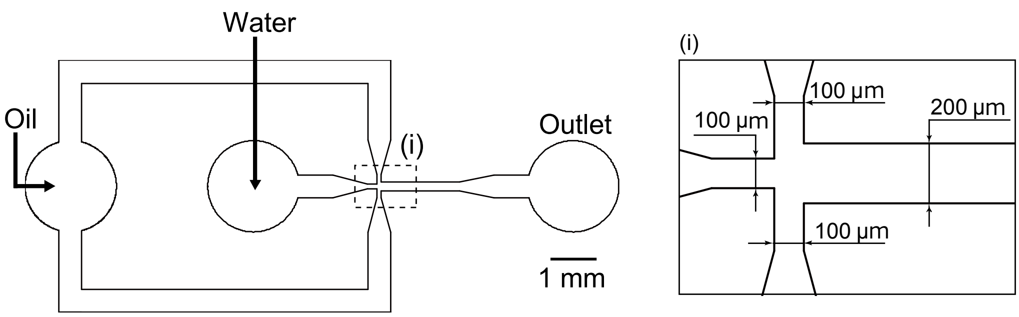


**Fig. S2** A schematic diagram showing the cross-shaped MFDG without a DLD region.

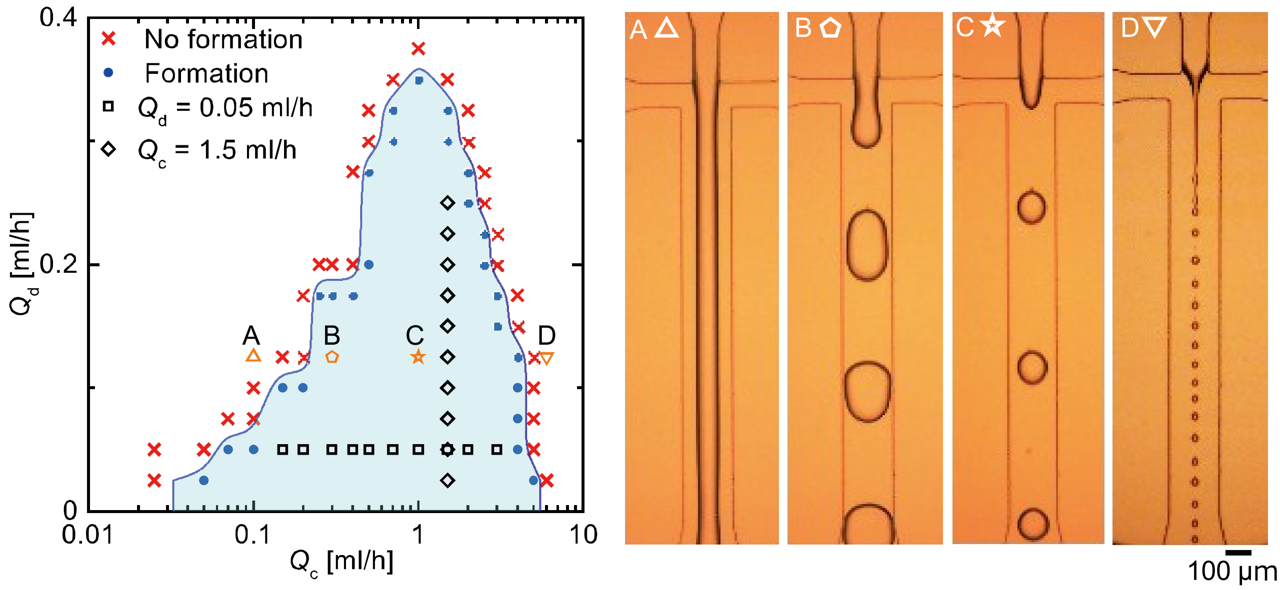


**Fig. S3** Flow pattern diagram showing where monodisperse droplets can be formed reproducibly. The horizontal axis is the flow rate of the continuous phase ($Q_c$) and the vertical axis is the flow rate of dispersed phase ($Q_d$). The crosses represent the flow conditions under which monodisperse droplets cannot be generated. The solid circles represent the flow conditions under which monodisperse droplets can be formed. The solid line shows the empirically estimated boundary at which the transition occurs between the flow regimes. The open triangle, pentagon, star and inverted triangle represent four different flow regimes (inset A, B, C and D) under four different $Q_c$ values and constant $Q_d$ (= 0.125 ml/h). The open squares and diamonds represent the flow conditions under which the sizes of main and satellite droplets were measured (see Fig. 3c and d).

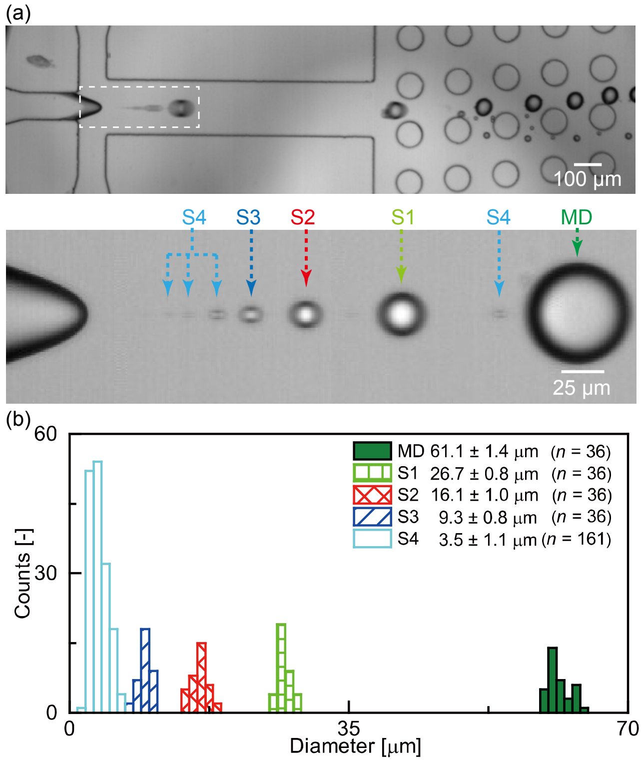


**Fig. S4** Formation of water-in-oil (W/O) main and satellite droplets in a device with a single DLD array. (a) Main (MD) and satellite (S1–S4) droplets immediately following their breakup. (b) Size distributions of main and satellite droplets. The flow rates were $Q_c = 3.0$ ml/h and $Q_d = 0.05$ ml/h. The break up rate was ~110 drops s $^{-1}$.

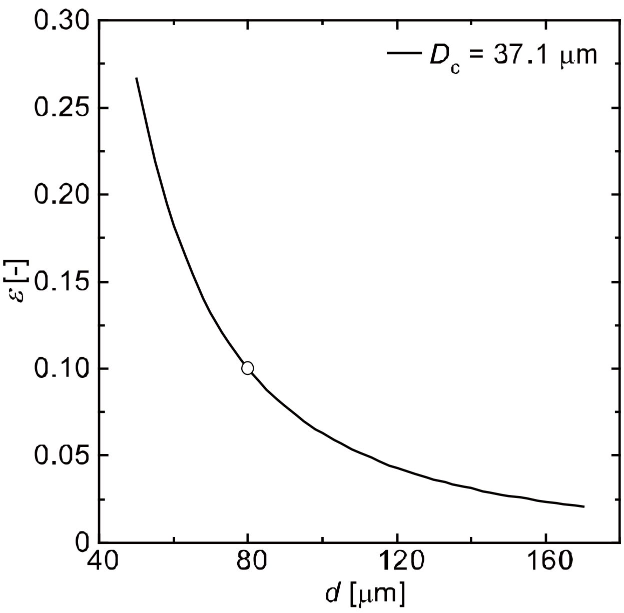


**Fig. S5** Relationship between a gap ($d$) and a row shift fraction ($\varepsilon$) at $D_c = 37.1$ µm. The open circle represents the DLD parameter of the Device-1, Device-2 and the first region of Device-3.

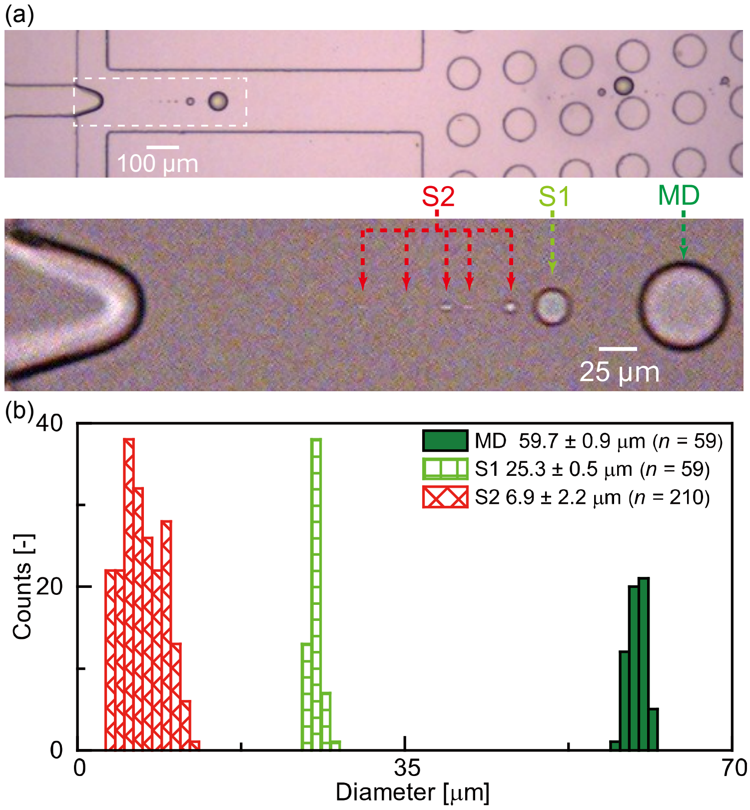


**Fig. S6** (a) Formation of oil-in-water (O/W) main and satellite droplets in a hydrophilic device with a single DLD region. The magnified image was captured at 37500 fps. The flow rates were $Q_c$ = 20.0 ml/h and $Q_d$ = 0.1 ml/h. The breakup rate of the main droplets was 214 drops s $^{-1}$. (b) Size distributions of the main and satellite droplets.

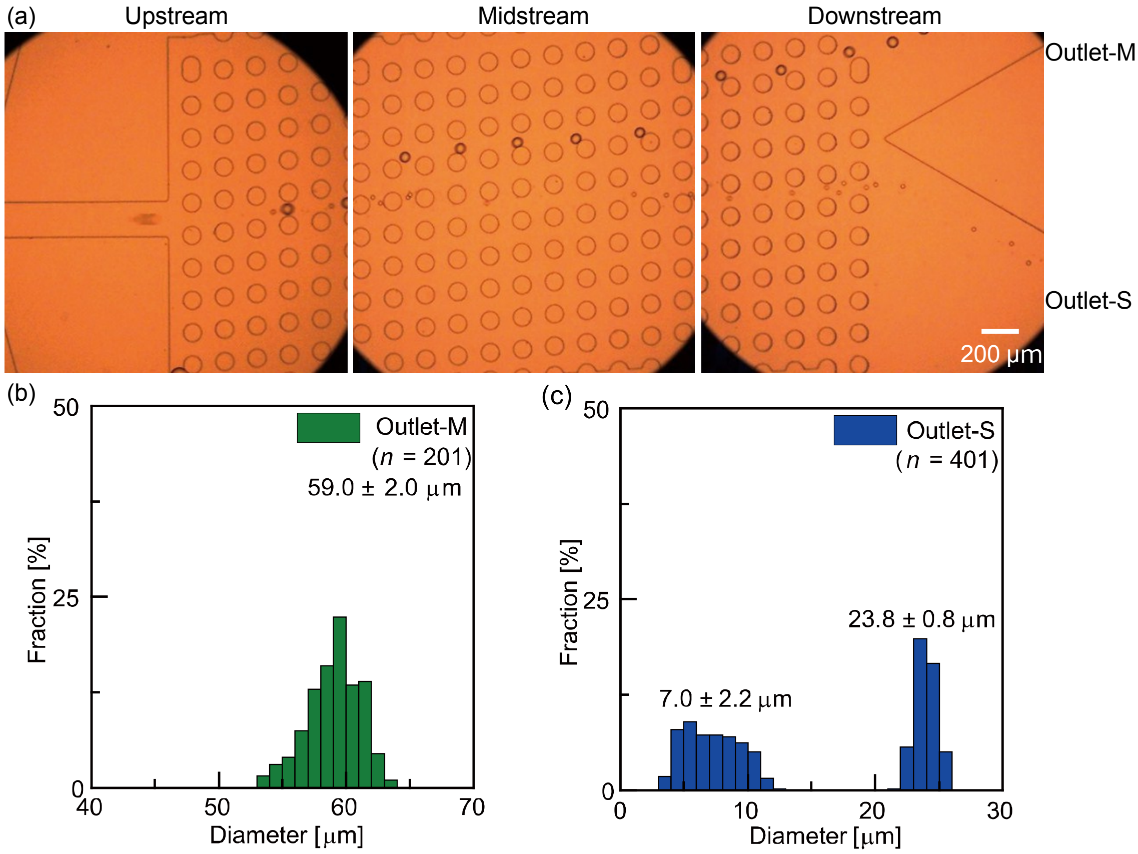


**Fig. S7** Separation of O/W main and satellite droplets through a hydrophilic single-step DLD array. (a) Photographs of the O/W main and satellite droplets flowing through the DLD pillars recorded at 5000 fps. The flow rates were $Q_d$ = 0.1 ml/h, $Q_c$ = 20.0 ml/h. (b, c) Size distributions of the collected droplets at (b) Outlet-M and (c) Outlet-S.

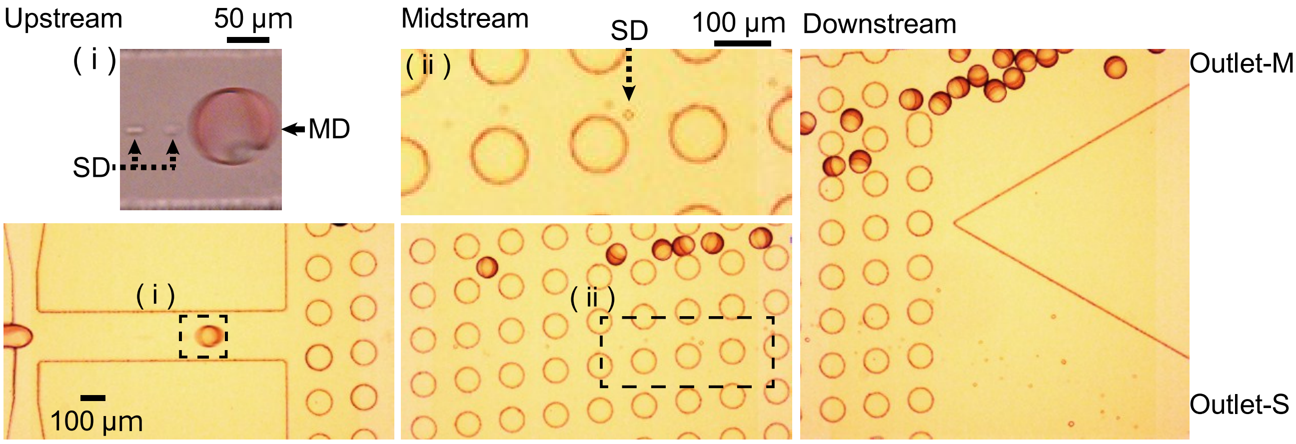


**Fig. S8** Photographs showing the separation of Janus main and satellite droplets flowing through the DLD array. The flow rates of the two disperse phases (monomer $Q_m$ and silicone oil $Q_s$) were $Q_m = Q_s = 0.1$ ml/h. $Q_c = 15.0$ ml/h. Dashed rectangles correspond to the photographs of magnified view.

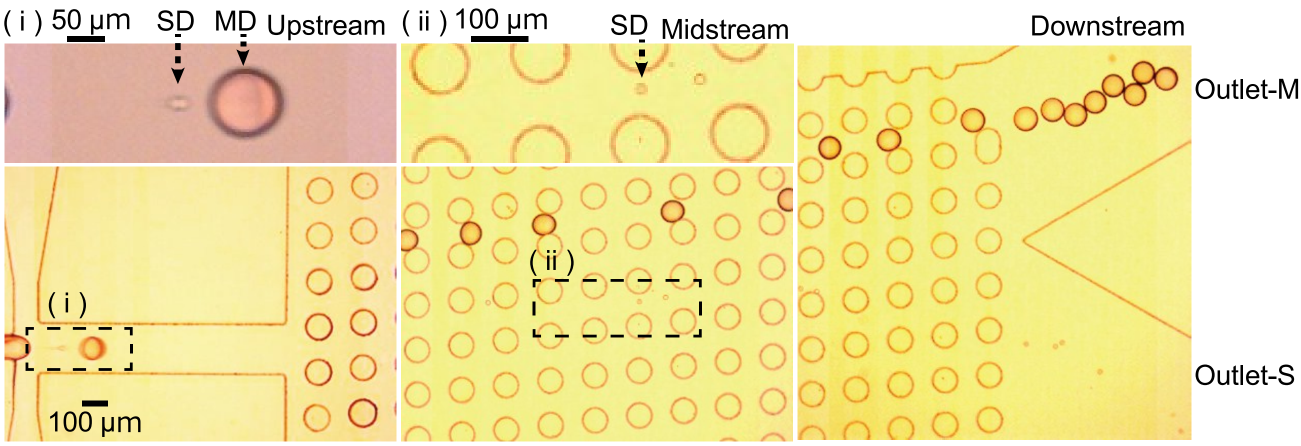


**Fig. S9** Photographs showing the separation of core-shell main and satellite droplets flowing through the DLD array. The flow rates were $Q_m = Q_s = 0.05$ ml/h, $Q_c = 15.0$ ml/h. Dashed rectangles correspond to the photographs of magnified view.

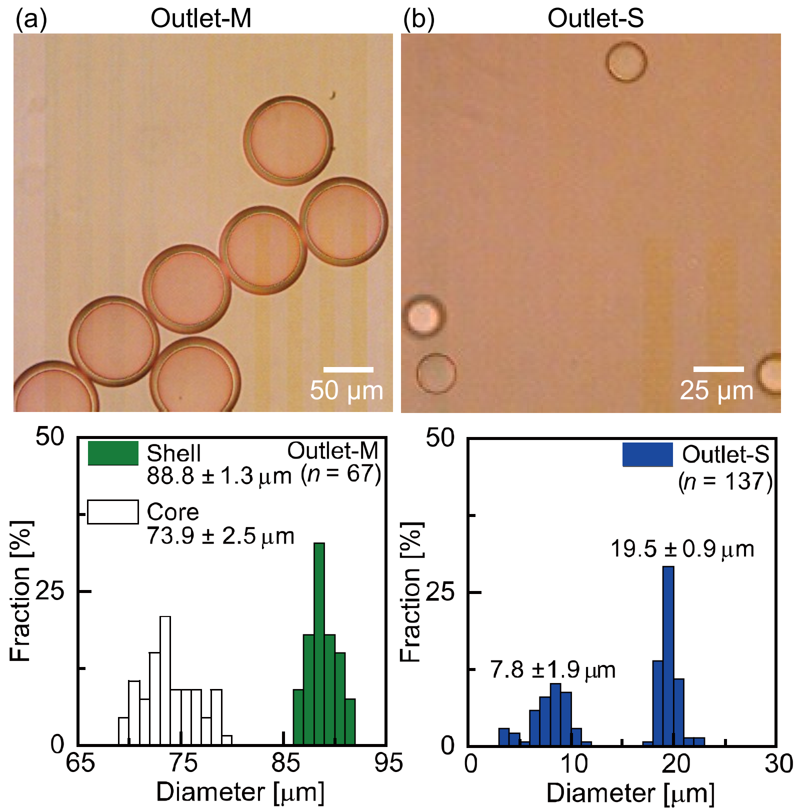


**Fig. S10** Photomicrographs and size distributions of the separated (a) main and (b) satellite core-shell droplets.

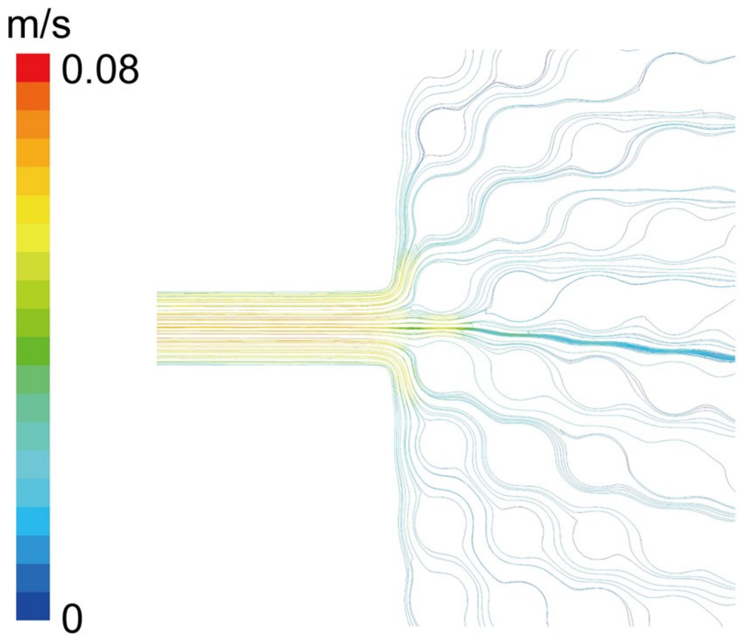


**Fig. S11** A result of three-dimensional flow simulation by a commercially-available software (ANSYS fluent), showing the streamlines from a MFDG drain channel to the expanded DLD array. Input flow rate is 3.05 ml/h.

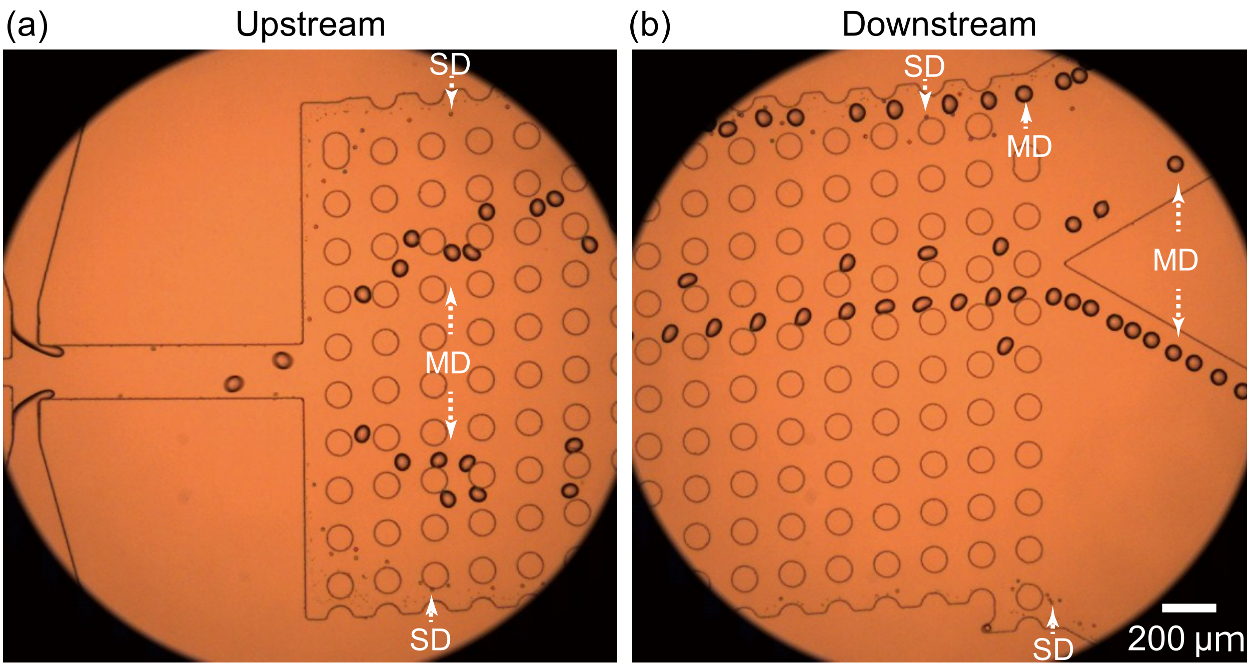


**Fig. S12** Alternate formation of W/O droplets at two opposed T-junctions and their trajectories through the DLD array. The flow rates were $Q_d$ = 0.1 ml/h, $Q_c$ = 3.0 ml/h.

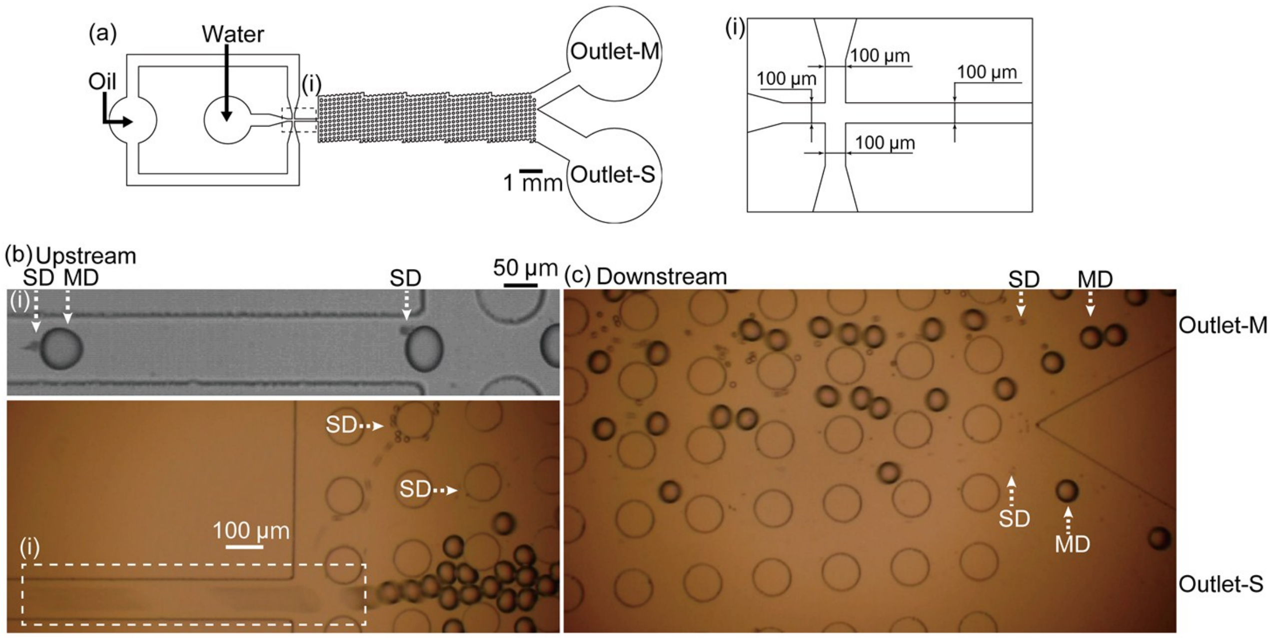


**Fig. S13** Effect of width of the entrance channel before the DLD region on the droplets separation. (a) Off-centered position of the satellite droplets flowing through the entrance channel of 100 μm width. (b, c) Resulting trajectories of the main and satellite droplets in the DLD region. The flow rates were $Q_d$ = 0.05 ml/h, $Q_c$ = 1.0 ml/h.

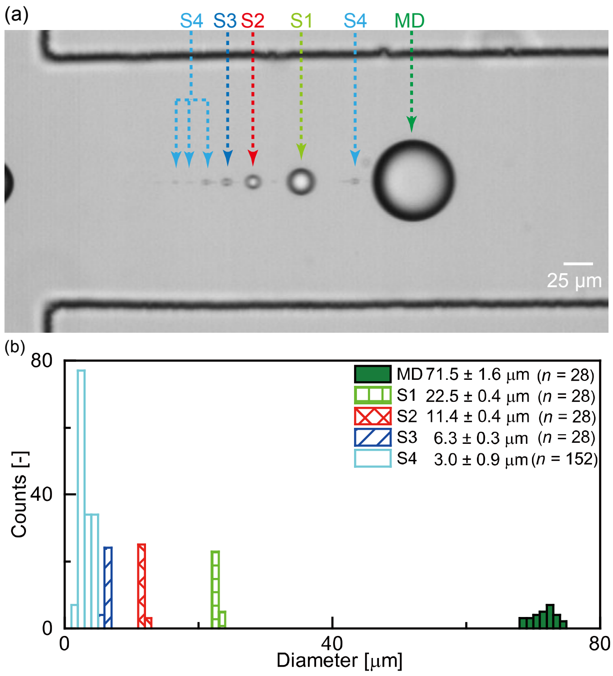


**Fig. S14** Formation of W/O main and satellite droplets in a MFDG leading to a three-step DLD array. (a) Main and satellite droplets immediately following their breakup. (b) Size distributions of main and satellite droplets. The flow rates were $Q_c$ = 3.0 ml/h and $Q_d$ = 0.05 ml/h. The break up rate was ~70 drops $s^{-1}$.

**Supplementary movie captions:**

01_dev_1a_up: Movie clip of the separation of W/O main and satellite droplets in the upstream Device-1A, recorded at 2000 fps (see Fig. 4).

02_dev_1a_mid: Movie clip of the separation of W/O main and satellite droplets in the midstream Device-1A, recorded at 2000 fps (see Fig. 4).

03_dev_1a_down: Movie clip of the separation of W/O main and satellite droplets in the downstream Device-1A, recorded at 2000 fps (see Fig. 4).

04_dev_3_rgn1: Movie clip of the separation of W/O main and satellite droplets through Region-1, recorded at 2000 fps (see Fig. 8).

05_ dev_3_rgn2: Movie clip of the separation of the largest satellite droplets (S1) from the smaller satellite droplets through Region-2, recorded at 2000 fps (see Fig. 8).

06_ dev_3_rgn3: Movie clip of the separation of the second largest satellite droplets (S2) from the other smaller satellite droplets (S3 and S4) through Region-3, recorded at 2000 fps (see Fig. 8).

All files are in MPEG-4 format.